

decrease in BPH angle as compared to that in the planar form of the neutral molecule is much more extreme than the change in BNH angle. Furthermore, the B-P bond length is longer in the anion than in the planar form of the neutral molecule (1.829 and 1.807 Å, respectively), while in the nitrogen compounds the B-N bond length is shorter in the anion. The B-H bond lengths are slightly shorter in BH_2PH^- than in BH_2NH^- , while the proton affinity of BH_2PH^- is substantially lower than that of BH_2NH^- (15.2 and 18.0 eV, respectively).

All 12 vibrational frequencies have been measured experimentally for the BH_2NH_2 molecule.²⁹ When these results are compared with our data in Table I for planar BH_2PH_2 , the most striking difference is of course the imaginary PH_2 wagging frequency versus 1005 cm^{-1} for the NH_2 wag. The BP stretching frequency of 827 cm^{-1} is much smaller than the BN stretch, 1337 cm^{-1} , but the torsion frequencies are about the same (723 cm^{-1} for the phosphorus-containing molecule and 763 cm^{-1} for the

nitrogen-containing molecule). Of the remaining nine frequencies, the four that primarily involve P or N are smaller for the phosphorus-containing molecule, averaging about 76% of the nitrogen-containing molecule's frequencies. On the other hand, four of the five frequencies that primarily involve B are larger in planar BH_2PH_2 . The largest difference is found with the BH_2 wag: 990 cm^{-1} for the phosphorus-containing molecule and 670 cm^{-1} for the nitrogen-containing molecule. However, the latter value as well as two other frequencies are estimates based on perturbations in another frequency.

Acknowledgment. We wish to express our thanks to Wesley D. Allen, Roger L. DeKock, William H. Fink, Philip P. Power, Gustavo E. Scuseria, and Yukio Yamaguchi for helpful discussions and to William H. Fink for the orbital contour diagrams. The research was supported by the U.S. Air Force Office of Scientific Research (AFOSR) under Grant AFOSR-87-0182.

Contribution from the Institut de Chimie Minérale et Analytique, Université de Lausanne, 3, Place du Château, CH-1005 Lausanne, Switzerland

Tetrasolventberyllium(II): High-Pressure Evidence for a Sterically Controlled Solvent-Exchange-Mechanism Crossover^{1,2}

Pierre-André Pittet, Gilles Elbaze, Lothar Helm, and André E. Merbach*

Received September 25, 1989

The kinetics of solvent S exchanges on tetrasolventberyllium(II) have been studied by variable-temperature and -pressure ¹H NMR spectroscopy with S = dimethyl sulfoxide (DMSO), trimethyl phosphate (TPMA), *N,N*-dimethylformamide (DMF), tetramethylurea (TMU), dimethylpropyleneurea (DMPU) or ¹⁷O NMR spectroscopy with S = H₂O. The nonaqueous solvent-exchange reactions were studied in the inert diluent nitromethane to allow the determination of the k_1 and k_2 terms contributing to the observed rate k_{obs} , according to $k_{\text{obs}} = k_1 + k_2[\text{S}]$. For DMSO and TPMA the second-order rate law ($k_1 = 0$) implies an interchange I or associative A mechanism, whereas for TMU and DMPU the first-order rate law ($k_2 = 0$) indicates a dissociative D mechanism. For DMF both k_1 and k_2 terms contribute to k_{obs} . The pseudo-first-order rate constant k_{ex} for water exchange in neat H₂O was obtained from measurements of the bound-water transverse relaxation rate in the presence of Mn^{2+} as a relaxation agent. The results were $k_{\text{ex}}^{298} = 733 \pm 56\text{ s}^{-1}$, $\Delta H^\ddagger = 59.2 \pm 1.5\text{ kJ mol}^{-1}$, $\Delta S^\ddagger = +8.4 \pm 4.5\text{ J K}^{-1}\text{ mol}^{-1}$, and $\Delta V^\ddagger = -13.6 \pm 0.5\text{ cm}^3\text{ mol}^{-1}$. In the absence of a rate law, the very negative value of the activation volume ΔV^\ddagger is interpreted in terms of an A mechanism. The negative values of ΔV^\ddagger for the k_2 path (-2.5 , -4.1 , and $-3.1\text{ cm}^3\text{ mol}^{-1}$ for S = DMSO, TPMA, and DMF) support evidence of an I_a or A mechanism, whereas the positive values of ΔV^\ddagger for the k_1 path ($+10.5$ and $+10.3\text{ cm}^3\text{ mol}^{-1}$ for S = TMU and DMPU) confirm the operation of a D mechanism. These data suggest together that a mechanism crossover is taking place, from associative A for the smallest H₂O to dissociative D for the bulky TMU and DMPU.

Introduction

It is apparent from previous nonaqueous studies,³⁻¹⁰ mainly from Lincoln's group, that the mode of activation for solvent exchange (eq 1) on the small tetrahedrally coordinated beryllium(II) ion



can vary from dissociative to associative depending upon the nature of the exchanging solvent. The mechanistic assignments⁸ were based on correlations between both the stereochemistry and the electron-donating power of the solvent S and its propensity to exchange through a first- and/or second-order pathway in non-

coordinating high-dielectric diluents, like nitromethane. Considering the success of high-pressure NMR spectroscopy in the elucidation of the mechanisms of solvent-exchange reactions on metal ions, in particular in showing a gradual mechanism changeover¹¹ along both series of divalent and trivalent high-spin first-row hexasolvated transition-metal ions, we have complemented the beryllium(II) nonaqueous solvent-exchange work by a high-pressure proton NMR study in the diluent nitromethane.

Further, the available variable-temperature data^{12,13} for water exchange on beryllium(II) are still subject to criticism. The recourse to manganese(II) as relaxation agent for the bulk-water oxygen-17 NMR signal, successfully used in the case of $[\text{Al}(\text{H}_2\text{O})_6]^{3+}$,¹⁴ $[\text{Ga}(\text{H}_2\text{O})_6]^{3+}$,¹⁵ and $[\text{Pd}(\text{H}_2\text{O})_4]^{2+}$,¹⁶ will be very helpful in obtaining accurate exchange rates in dilute solutions. Moreover, in this case where no rate law is available due to the lack of a suitable diluent for water, the determination of the activation volume is essential for the assignment of the water-

- (1) High-Pressure NMR Kinetics. 44. For part 43, see ref 2. Taken, in part, from the Ph.D. thesis of P.-A. P.
- (2) Turin-Rossier, M.; Hugi-Cleary, D.; Frey, U.; Merbach, A. E. *Inorg. Chem.* **1990**, *29*, 1374.
- (3) Lincoln, S. F.; Tkaczuk, M. N. *Ber. Bunsen-Ges. Phys. Chem.* **1981**, *85*, 433.
- (4) Földner, H. H.; Devia, D. H.; Strehlow, H. *Ber. Bunsen-Ges. Phys. Chem.* **1978**, *82*, 499.
- (5) Delpuech, J. J.; Péguy, A.; Rubini, P.; Steinmetz, J. *Nouv. J. Chim.* **1977**, *1*, 133.
- (6) Crea, J.; Lincoln, S. F. *J. Chem. Soc., Dalton Trans.* **1973**, 2075.
- (7) Tkaczuk, M. N.; Lincoln, S. F. *Ber. Bunsen-Ges. Phys. Chem.* **1982**, *86*, 147.
- (8) Lincoln, S. F.; Tkaczuk, M. N. *Ber. Bunsen-Ges. Phys. Chem.* **1982**, *86*, 221.
- (9) Tkaczuk, M. N.; Lincoln, S. F. *Aust. J. Chem.* **1982**, *35*, 1555.
- (10) Matwiyoff, N. A.; Movius, W. G. *J. Am. Chem. Soc.* **1967**, *89*, 6077.

- (11) Merbach, A. E. *Pure Appl. Chem.* **1987**, *59*, 161.
- (12) Neely, J. W. Ph.D. Thesis, University of California, Berkeley, 1971; Report UCLR-20580.
- (13) Frahm, J.; Földner, H. H. *Ber. Bunsen-Ges. Phys. Chem.* **1980**, *84*, 173.
- (14) Hugi-Cleary, D.; Helm, L.; Merbach, A. E. *Helv. Chim. Acta* **1985**, *68*, 545.
- (15) Hugi-Cleary, D.; Helm, L.; Merbach, A. E. *J. Am. Chem. Soc.* **1987**, *109*, 4444.
- (16) Helm, L.; Elding, L. I.; Merbach, A. E. *Helv. Chim. Acta* **1984**, *67*, 1453.

Table I. Observed Exchange Rate, k_{obs} , and Deduced Rate Constants, k_1 and k_2 , for Solvent S Exchange on BeS_4^{2+} at Different Concentrations of Solvent S, in CD_3NO_2 as Diluent, at Constant Temperature and Ambient Pressure

DMSO ^a		DMF ^b		TMU ^c		DMPU ^d		
[S]/ mol kg ⁻¹	$k_{\text{obs}}/\text{s}^{-1}$	[S]/ mol kg ⁻¹	$k_{\text{obs}}/\text{s}^{-1}$	[S]/ mol kg ⁻¹	$k_{\text{obs}}/\text{s}^{-1}$	[S]/ mol kg ⁻¹	$k_{\text{obs}}/\text{s}^{-1}$	$k_{\text{obs}}/\text{s}^{-1}$
0.0302	6.3	0.054	61.0	0.106	57.2	0.068	11.7	39.1
0.0794	11.6	0.194	137.0	0.239	57.6	0.087	12.6	40.6
0.179	20.6	0.407	249.0	0.433	59.1	0.184	12.5	37.2
0.364	38.9			0.608	57.8	0.444	12.7	38.3
0.636	65.0			1.316	59.6	1.107	12.0	38.5
1.360	151.5					2.027	12.6	38.0
k_1/s^{-1}	(-3.0 ± 3.1)		33.0 ± 0.7		57.4 ± 0.8		12.2 ± 0.4	38.7 ± 0.6
$k_2/\text{kg mol}^{-1} \text{s}^{-1}$	110.5 ± 1.4		531.6 ± 2.5		(1.7 ± 0.8)		(0.2 ± 0.2)	(-0.3 ± 0.4)

^aAt 286.2 K; $[\text{Be}(\text{DMSO})_4^{2+}] = 0.083 \text{ mol kg}^{-1}$; $\delta_F = 2.57 \text{ ppm}$; $\delta_C = 3.01 \text{ ppm}$ (F = free solvent; C = coordinated solvent). ^bAt 355.1 K; $[\text{Be}(\text{DMF})_4^{2+}] = 0.049 \text{ mol kg}^{-1}$; $\delta_F = 2.79, 2.94$ (N-methyls), 7.88 ppm (formyl); $\delta_C = 3.11, 3.23$ (N-methyls), 8.08 ppm (formyl). ^cAt 337.3 K; $[\text{Be}(\text{TMU})_4^{2+}] = 0.097 \text{ mol kg}^{-1}$; $\delta_F = 2.75 \text{ ppm}$; $\delta_C = 3.00 \text{ ppm}$. ^dAt 338.3 and 351.7 K; $[\text{Be}(\text{DMPU})_4^{2+}] = 0.101 \text{ mol kg}^{-1}$; $\delta_F = 2.83$ (N-methyls), 3.26 ppm (t, $J(^1\text{H}-^1\text{H}) = 6.0 \text{ Hz}$, H β to the carbonyl); $\delta_C = 3.07$ (N-methyls), 3.43 ppm (t, $J(^1\text{H}-^1\text{H}) = 5.7 \text{ Hz}$, H β to the carbonyl). ^eFor $[\text{Be}(\text{TMP})_4]^{2+}$: $\delta_F = 3.72 \text{ ppm}$ (d, $J(^1\text{H}-^31\text{P}) = 36 \text{ Hz}$); $\delta_C = 4.01 \text{ ppm}$ (d, $J(^1\text{H}-^31\text{P}) = 38 \text{ Hz}$).

exchange mechanism on the aquaberyllium(II) ion.

Experimental Section

Materials and Preparation of Solutions. Beryllium oxide (Fluka, purum), perchloric acid (Merck, p.a.), $\text{Mn}(\text{ClO}_4)_2$ (Fluka, p.a.), NaClO_4 (Merck, p.a.), triethyl orthoformate (Fluka, puriss), deuterated nitromethane (Ciba-Geigy), and oxygen-17-enriched water (Yeda, 15–40 atom %, ^1H normalized) were used without further purification. Hydrated aluminum perchlorate (Fluka, purum) and gallium perchlorate (Ventron, puriss) were dried in vacuo (10^{-2} Torr) overnight. *N,N*-dimethylformamide (DMF), tetramethylurea (TMU), dimethylpropyleneurea (DMPU), dimethyl sulfoxide (DMSO), and trimethyl phosphate (TMP) (all Fluka, puriss) were dried over 4-Å molecular sieves.

Hydrated beryllium perchlorate was obtained by heating beryllium oxide under reflux in an excess of HClO_4 , 40%, filtering the solution and evaporating it until precipitation. The salt was collected by filtration and dried in vacuo (10^{-2} Torr) overnight. $[\text{Be}(\text{DMSO})_4](\text{ClO}_4)_2$, $[\text{Be}(\text{TMP})_4](\text{ClO}_4)_2$, $[\text{Be}(\text{DMF})_4](\text{ClO}_4)_2$, $[\text{Be}(\text{TMU})_4](\text{ClO}_4)_2$, and $[\text{Be}(\text{DMPU})_4](\text{ClO}_4)_2$ were prepared under N_2 by the following procedure. A 5.4-mmol sample of hydrated beryllium perchlorate was dissolved in 20 g of triethyl orthoformate, the solution was stirred for 2 h at room temperature, and then 34.5 mmol of the desired solvent was added. Precipitation of the solvate was induced by concentration under reduced pressure and addition of dry diethyl ether where necessary. The solid was washed with diethyl ether and then dried in vacuo (10^{-4} Torr) overnight. Anal. Calcd for $[\text{Be}(\text{DMPU})_4](\text{ClO}_4)_2$: C, 39.73; H, 6.60; N, 15.51; Cl, 9.97; Be, 1.57. Found: C, 40.0; H, 6.71; N, 15.55; Cl, 9.84; Be, 1.25. The analyses of the other products agreed also with the theoretical formulas. Hydrated rhodium perchlorate was prepared in accordance with the synthesis of Ayres and Forrester¹⁷ and its composition determined by elementary analysis. Solutions in CD_3NO_2 as inert diluent were prepared by weight in a glovebox. All concentrations were expressed in moles per kilogram of solvent (mol kg^{-1}). The internal ^1H NMR chemical shift reference was 5% w/w TMS.

The precise water content of the salts used in the aqueous solution studies was determined by Karl Fischer titration and also by ion-exchange chromatography (Dowex 50W-X8 resin, H^+ form) followed by titration of the liberated H^+ . The ionic strength (1.0 mol kg^{-1}) was kept constant by use of NaClO_4 , and no diluent was added.

The solutions used for the determination of the coordination number of Be^{2+} (Al^{3+} , Ga^{3+} , respectively) in water were $0.104 \text{ mol kg}^{-1}$ metal perchlorate (0.201, 0.201), 1.00 mol kg^{-1} HClO_4 , 0.12 mol kg^{-1} $\text{Mn}(\text{ClO}_4)_2$ (0.50, 0.50), and $0.073 \text{ mol kg}^{-1}$ rhodium perchlorate (0.218, 0.221), in 10% ^{17}O -enriched water. They were prepared by weight and heated at 373 K in sealed tubes for 48 h to allow complete ^{17}O equilibrium between the bulk and the coordinated water, even for the slow-exchanging $[\text{Rh}(\text{H}_2\text{O})_6]^{3+}$.¹⁸

Proton NMR Measurements. Spectra were recorded on a Bruker CXP-200 spectrometer (cryomagnet, 4.7 T) working at 200 MHz. For variable-temperature study, samples in 5 mm o.d. sealed tubes were thermostated with a flux of nitrogen and the temperature was measured by a substitution technique.¹⁹ The field was locked by using the deuterium signal of the diluent. Variable-pressure measurements were

performed with the high-pressure probe described previously,²⁰ without lock. A built-in platinum resistor allows temperature measurement, with an accuracy of $\pm 1 \text{ K}$ after all corrections.²¹ The sweep width was 2000 Hz, the number of scans varied from 30 to 60, and the repetition rate varied from 10 to 20 s. Spectra were recorded by using 4–32K data points. Chemical shifts were referred to TMS, which was also used to estimate inhomogeneity corrections.

Oxygen-17 NMR Measurements. Variable-temperature spectra were obtained on a Bruker AM-400 spectrometer working at 54.3 MHz. Samples in 10 mm o.d. tubes were investigated from 267 to 352 K. Thermostating and temperature measurement were as described above. The pressure study was done on the CXP-200 spectrometer with the high-pressure probe tuned at 27.1 MHz. The ClO_4^- signal was minimized by pulsing rapidly at its resonance. The sweep width varied from 20 to 100 kHz, the number of data points from 1024 to 4096, and the number of scans from 10^4 to 1.5×10^6 with a pulse length of 14 μs . Oxygen-17 enrichment was 15% (AM-400) and 40% (CXP-200). Before Fourier transformation, the data points were treated with an exponential filter function, resulting in line broadening of approximately 5% of $\Delta\nu_{1/2}$, the signal width at half-height. The NMR signal was fitted to a Lorentzian line shape, and the transverse relaxation rate of the bound water, $1/T_2^b$, was determined from $\Delta\nu_{1/2}$, after correction for the line broadening.

Computation Method. The analysis of the experimental data using the required equations was done by a nonlinear least-squares program fitting the desired parameters values. Reported errors are 1 standard deviation.

Results and Data Treatment

Nonaqueous Solvent Exchange. Under slow exchange the ^1H NMR spectra of deuterated nitromethane solutions of $[\text{BeS}_4](\text{ClO}_4)_2$ in the presence of an excess of solvent S (S = DMSO, TMP, DMF, TMU, and DMPU) consist of two signals, one at high frequency due to the solvent molecules in the primary coordination sphere of Be^{2+} and one at low frequency due to the free solvent. By comparison of the bound and free solvent peaks areas, a coordination number of 4.0 ± 0.1 was determined for the Be^{2+} nonaqueous solvates studied.

At increasing temperatures coalescence of the resonances of the coordinated and the free solvent molecules occurs as a consequence of the intermolecular solvent-exchange reaction (eq 1). The calculated spectra were least-squares fitted to the observed spectra, by using a program derived from EXCHNG.²² The concentrations, chemical shifts, and coupling constants used in the calculations are given in Table I. The full spectra were analyzed for TMU, DMSO, and TMP. For the DMF exchange, only the signals due to the methyl groups were taken into account. For the DMPU variable-temperature work, only the methyl groups were used whereas, for the variable-pressure work, the triplets arising from the methylene groups β to the carbonyl had to be included in the analysis, because at the temperature chosen, these triplets were overlapping the methyl singlets.

(17) Ayres, G. H.; Forrester, J. S. *J. Inorg. Nucl. Chem.* **1957**, *3*, 365.

(18) Rapaport, I. Ph.D. Thesis, University of Lausanne, Switzerland, 1987.

(19) Ammann, C.; Meier, P.; Merbach, A. E. *J. Magn. Reson.* **1982**, *46*, 319.

(20) Pisaniello, D. L.; Helm, L.; Meier, P.; Merbach, A. E. *J. Am. Chem. Soc.* **1983**, *105*, 4258.

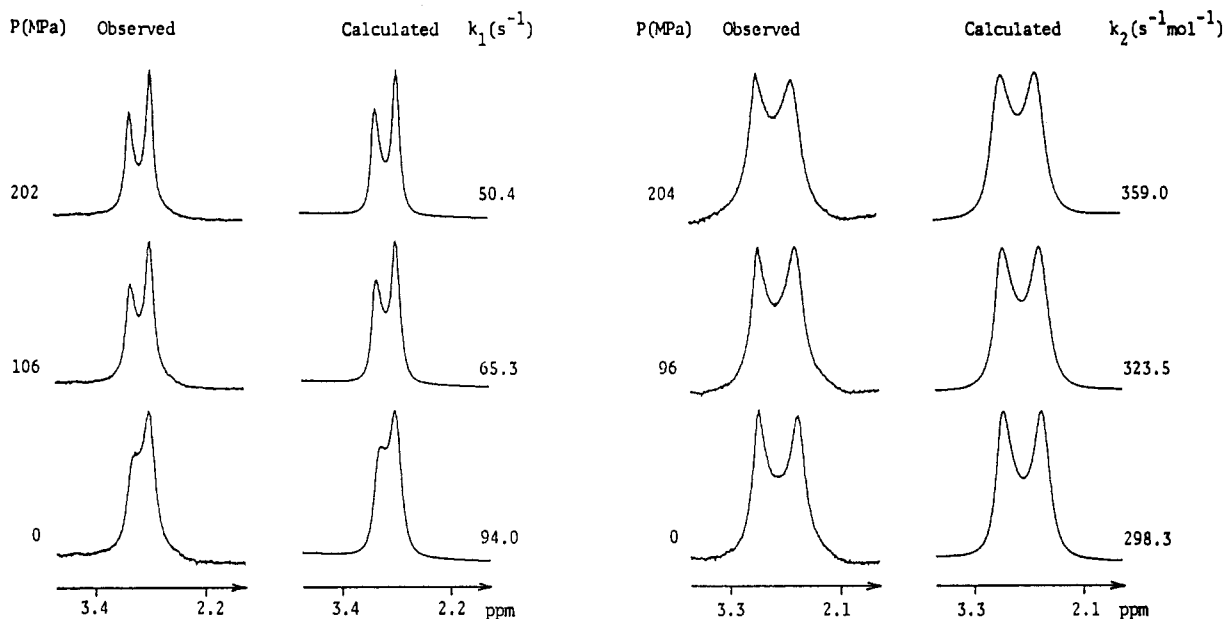
(21) Meyer, F. K.; Merbach, A. E. *J. Phys. E* **1979**, *12*, 185.

(22) Delpuech, J. J.; Ducom, J.; Michon, V. *Bull. Soc. Chim. Fr.* **1971**, 1848.

Table II. Temperature Dependence of the First- and Second-Order Rate Constants, k_1 and k_2 , Respectively, and Deduced Kinetic Parameters for Solvent S Exchange on BeS_4^{2+} in CD_3NO_2 as Diluent

DMSO ^a		TMP ^b		DMF ^c			TMU ^d		DMPU ^e	
T/K	$k_2/\text{kg mol}^{-1} \text{ s}^{-1}$	T/K	$k_2/\text{kg mol}^{-1} \text{ s}^{-1}$	T/K	k_1/s^{-1}	$k_2/\text{kg mol}^{-1} \text{ s}^{-1}$	T/K	k_1/s^{-1}	T/K	k_1/s^{-1}
247.8	10.1	311.3	10.2	305.6		25.3	305.6	2.7	246.1	1.3
258.7	22.5	314.1	11.8	314.3		53.2	314.3	4.7	300.9	2.1
269.6	41.7	321.6	16.3	321.8	2.1	78.9	321.8	11.0	322.2	3.1
278.6	74.7	331.8	25.9	330.2	3.4	138.8	330.2	25.8	337.7	9.2
289.7	139.6	337.5	34.3	338.7	8.0	235.3	338.7	56.0	344.9	22.7
305.6	295.6	342.0	41.8	347.0	21.1	323.0	347.0	110.0	353.1	44.6
314.3	446	352.0	69.2	355.1	33.0	531.6	355.1	214.0	361.6	93.8
321.8	642	362.1	115.8	363.2	45.0	856.7	363.2	393.0	371.8	234.6
330.2	914	367.3	162.9						377.0	334.9
338.7	1356	372.3	180.1							
347.0	1891									
k_1^{298}/s^{-1}					0.2 ± 0.1			1.0 ± 0.1		0.1 ± 0.02
$k_2^{298}/\text{kg mol}^{-1} \text{ s}^{-1}$	213.0 ± 2.3	4.2 ± 0.3				15.9 ± 0.9				
$\Delta H^\ddagger/\text{kJ mol}^{-1}$	35.0 ± 0.2	43.5 ± 1.5			74.9 ± 6.4	52.0 ± 1.2		79.6 ± 2.0		92.6 ± 2.6
$\Delta S^\ddagger/\text{J K}^{-1} \text{ mol}^{-1}$	-83.0 ± 0.8	-87.1 ± 3.9			-7.3 ± 18.6	-47.5 ± 3.7		$+22.3 \pm 5.8$		$+47.5 \pm 7.4$

^a $[\text{Be}(\text{DMSO})_4^{2+}] = 0.107 \text{ mol kg}^{-1}$; $[\text{DMSO}] = 0.475 \text{ mol kg}^{-1}$. ^b $[\text{Be}(\text{TMP})_4^{2+}] = 0.100 \text{ mol kg}^{-1}$; $[\text{TMP}] = 0.421 \text{ mol kg}^{-1}$. ^c $[\text{Be}(\text{DMF})_4^{2+}] = 0.049 \text{ mol kg}^{-1}$; $[\text{DMF}] = 0.054, 0.194, 0.407 \text{ mol kg}^{-1}$. k_1 and k_2 were calculated from k_{obs} at each temperature by use of eq 2. ^d $[\text{Be}(\text{TMU})_4^{2+}] = 0.106 \text{ mol kg}^{-1}$; $[\text{TMU}] = 0.436 \text{ mol kg}^{-1}$. ^e $[\text{Be}(\text{DMPU})_4^{2+}] = 0.100 \text{ mol kg}^{-1}$; $[\text{DMPU}] = 0.406 \text{ mol kg}^{-1}$.

**Figure 1.** Observed and calculated 200-MHz ^1H NMR spectra for TMU (left) and DMSO (right) exchanges on Be^{2+} at different pressures (composition of the solutions as in Table III).

In the inert diluent nitromethane, the observed rate constant, k_{obs} , for the exchange of a particular solvent molecule S, may be related to a first- or second-order, or even mixed, rate law (eq 2), depending on the reaction mechanism. The k_{obs} values obtained

$$k_{\text{obs}} = k_1 + k_2[\text{S}] \quad (2)$$

as a function of free-solvent concentration were analyzed by using eq 2 (Table I). One-term rate laws were found for DMPU, TMU (both first order, $k_2 = 0$), and DMSO (second order, $k_1 = 0$). Both k_1 and k_2 terms contribute to k_{obs} for DMF, and their values were determined at each temperature from three free-solvent concentrations (Table II). For TMP we assumed a pure second-order rate law ($k_{\text{obs}} = k_2[\text{TMP}]$), as previously observed.⁵

The activation enthalpy and entropy, ΔH^\ddagger and ΔS^\ddagger , were obtained by measuring the temperature dependence of the rate constants and fitting¹⁴ the results to the Eyring equation (Table II).

Figure 1 shows the pressure effect on ^1H NMR spectra for TMU and DMSO exchanges on the tetrahedral BeS_4^{2+} in deuterated nitromethane at constant temperature. In the DMSO case the signals coalesce with increasing pressure, indicating an increase of the exchange rate. The acceleration of the exchange process

with pressure can be related to a bond-making-controlled process, whereas for TMU the reverse sequence of spectral behavior is indicative of a bond-breaking-controlled process. The pressure dependence of $\ln k$ can be described by the quadratic equation (3), where ΔV^\ddagger and k_0 are respectively the volume of activation

$$\ln k_P = \ln k_0 - P\Delta V^\ddagger/RT + \Delta\beta^*P^2/2RT \quad (3)$$

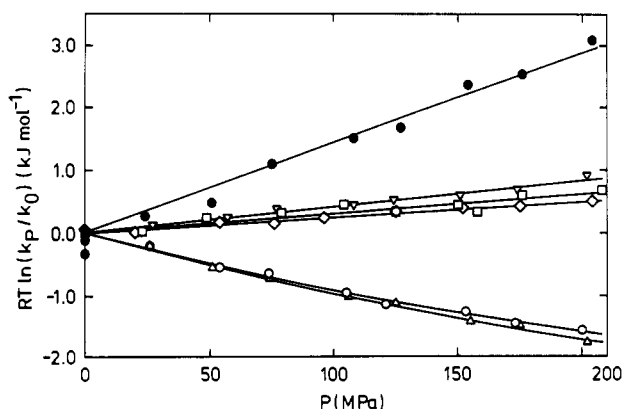
and the exchange rate constant, both at zero pressure, and $\Delta\beta^*$ is the compressibility coefficient of activation.²³ The results of the variable-pressure study are shown in Table III and in Figure 2. Note that for DMSO, TMP, and DMF exchanges the $\Delta\beta^*$ values are equal to zero within experimental errors: a linear fit was therefore used to calculate ΔV^\ddagger in these three cases.

Oxygen-17 Spectra of Aqueous Be^{2+} . If chemical exchange is slow, the ^{17}O NMR spectrum of a dilute aqueous solution containing an aquated metal ion consists of two resonances: a large, intense peak due to bulk H_2O and a smaller peak due to the $[\text{M}(\text{H}_2\text{O})_n]^{2+}$. In the case of Be^{2+} , the chemical shift between

Table III. Calculated Rate Constants at Zero Pressure and Activation Volumes ΔV^\ddagger for Solvent S Exchange on BeS_4^{2+} (in CD_3NO_2 as Diluent)

solvent	$(k_1)_0/s^{-1}$	$(k_2)_0/kg\ mol^{-1}\ s^{-1}$	$\Delta V^\ddagger/cm^3\ mol^{-1}$	$10^2\Delta\beta^\ddagger/cm^3\ mol^{-1}\ MPa^{-1}$	T/K
DMSO ^a		294.2 ± 2.7	-2.5 ± 0.2		300
TMP ^b		164.3 ± 1.2	-4.1 ± 0.2		371
DMF ^c		124.6 ± 2.3	-3.1 ± 0.4		326
TMU ^d	93.0 ± 0.9		$+10.5 \pm 0.7$	$+2.0 \pm 0.7$	346
DMPU ^e	68.4 ± 0.8		$+10.3 \pm 0.8$	$+2.4 \pm 0.9$	358

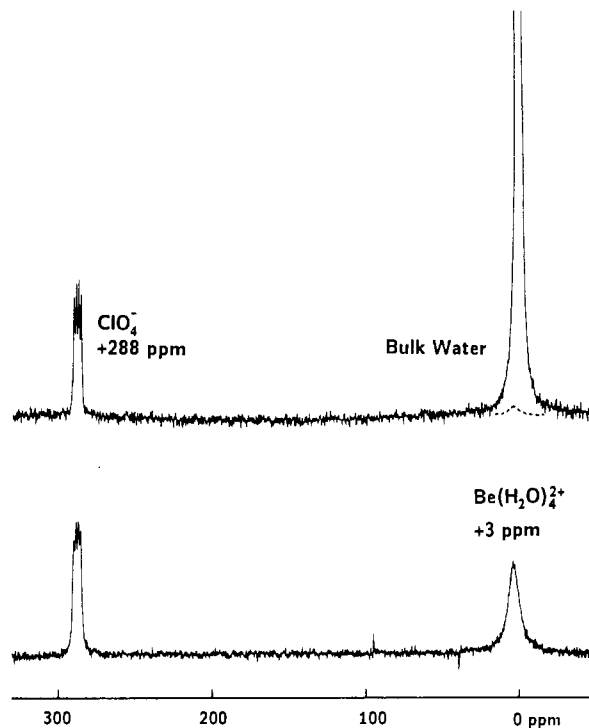
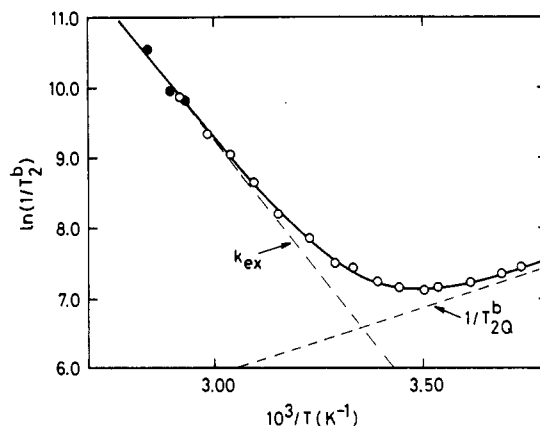
^a $[\text{Be}(\text{DMSO})_4^{2+}] = 0.103\ \text{mol}\ \text{kg}^{-1}$; $[\text{DMSO}] = 0.416\ \text{mol}\ \text{kg}^{-1}$.
^b $[\text{Be}(\text{TMP})_4^{2+}] = 0.102\ \text{mol}\ \text{kg}^{-1}$; $[\text{TMP}] = 0.404\ \text{mol}\ \text{kg}^{-1}$.
^c $[\text{Be}(\text{DMF})_4^{2+}] = 0.108\ \text{mol}\ \text{kg}^{-1}$; $[\text{DMF}] = 0.463\ \text{mol}\ \text{kg}^{-1}$; at these concentrations and temperature conditions $k_1 \ll k_2[\text{DMF}]$.
^d $[\text{Be}(\text{TMU})_4^{2+}] = 0.095\ \text{mol}\ \text{kg}^{-1}$; $[\text{TMU}] = 0.432\ \text{mol}\ \text{kg}^{-1}$.
^e $[\text{Be}(\text{DMPU})_4^{2+}] = 0.101\ \text{mol}\ \text{kg}^{-1}$; $[\text{DMPU}] = 0.421\ \text{mol}\ \text{kg}^{-1}$.

**Figure 2.** Pressure effect on the normalized natural logarithm of the rate constant for solvent exchange k_{ex} ($\text{H}_2\text{O} = \bullet$), k_2 (TMP = ∇ , DMF = \square , DMSO = \diamond), or k_1 (DMPU = \circ , TMU = \triangle) on BeS_4^{2+} (temperature and composition of the solutions as in Table III and Figure 5).

these two signals is small compared to their line widths. A natural-abundance ^{17}O spectrum of an acidified $\text{Be}(\text{ClO}_4)_2$ solution consists of a narrow, intense signal due to bulk H_2O at 0 ppm and a quadruplet due to ClO_4^- at +288 ppm (Figure 3, top). The bound- H_2O signal (dashed line), hidden under the large bulk water peak, is invisible on this spectrum. The addition of Mn^{2+} , a very efficient relaxation agent for the bulk signal due to its long electron relaxation time and its very fast coordinated-water/bulk-water exchange rate, results in an extremely broad bulk-water peak with negligible amplitude, revealing the underlying kinetically interesting bound-water signal (Figure 3, bottom). Previous experiments have shown that Mn^{2+} has no measurable effect on the bound-water transverse relaxation rate.¹⁶

Determination of the Coordination Number of Be^{2+} in Water.

The coordination number of Be^{2+} in water has already been investigated by ^{17}O NMR spectroscopy, using Co^{2+} ²⁴ or Eu^{3+} ¹³ as shift reagents for the bulk-water signal, or by a molal-shift method.²⁵ In each case, the number was found to be 4. However, a recent study by Yamaguchi et al.,²⁶ involving both molecular dynamics computer simulations and X-ray diffraction, yielded conflicting results, with coordination numbers of 6 and 4, respectively. All previously reported oxygen-17 NMR results were obtained in rather concentrated solutions. New measurements were performed by using Mn^{2+} as relaxation agent for the bulk-water signal, and in more dilute solutions as employed for the water-exchange study. The Rh^{3+} aqua ion was chosen as an internal oxygen-17 intensity reference, its coordination number being well-known to be 6.²⁷ Moreover, the resonance of $[\text{Rh}(\text{H}_2\text{O})_6]^{3+}$ ($\delta \approx +155$ ppm) is well separated from that of the aqua ion of Be^{2+} . This method was checked by determining the coordination numbers in water of Al^{3+} ^(6^{24,25,28}) and Ga^{3+} ^(6²⁸⁻³⁰). Determinations of the resonance integrals gave coordination numbers 6.0 ± 0.2 for Al^{3+} ($T = 327\ \text{K}$), 6.1 ± 0.2 for Ga^{3+} ($T = 295\ \text{K}$), and 4.1 ± 0.2 for Be^{2+} ($T = 295\ \text{K}$).

**Figure 3.** 54.24-MHz ^{17}O NMR spectra of an aqueous solution of $\text{Be}(\text{ClO}_4)_2$ ($0.10\ \text{mol}\ \text{kg}^{-1}$) with HClO_4 ($0.40\ \text{mol}\ \text{kg}^{-1}$) at 298 K: top, in normal water (0.037% ^{17}O), without Mn^{2+} ; bottom, in enriched water (0.40% ^{17}O), with $0.10\ \text{mol}\ \text{kg}^{-1}$ added $\text{Mn}(\text{ClO}_4)_2$.**Figure 4.** Temperature dependence on the transverse relaxation rate, $1/T_2^b$, of the bound- H_2O ^{17}O NMR signal of $0.1\ \text{mol}\ \text{kg}^{-1}$ $\text{Be}(\text{H}_2\text{O})_4^{2+}$ in 15% ^{17}O -enriched water, with $0.1\ \text{mol}\ \text{kg}^{-1}$ added $\text{Mn}(\text{ClO}_4)_2$ and various HClO_4 concentrations: \bullet , $0.38\ \text{mol}\ \text{kg}^{-1}$; \circ , mean value for 0.10, 0.20, and $0.38\ \text{mol}\ \text{kg}^{-1}$ solutions (measured at 54.24 MHz).

$(\text{H}_2\text{O})_6]^{3+}$ ($\delta \approx +155$ ppm) is well separated from that of the aqua ion of Be^{2+} . This method was checked by determining the coordination numbers in water of Al^{3+} ^(6^{24,25,28}) and Ga^{3+} ^(6²⁸⁻³⁰). Determinations of the resonance integrals gave coordination numbers 6.0 ± 0.2 for Al^{3+} ($T = 327\ \text{K}$), 6.1 ± 0.2 for Ga^{3+} ($T = 295\ \text{K}$), and 4.1 ± 0.2 for Be^{2+} ($T = 295\ \text{K}$).

Temperature Dependence of Water Exchange. Within the slow-exchange limits, the transverse relaxation rate of the oxygen-17 of water bound to a diamagnetic cation, $1/T_2^b$, is given by eq 4, where k_{ex} is the pseudo-first-order rate constant for the

$$1/T_2^b = k_{ex} + 1/T_{2Q}^b \quad (4)$$

exchange of a particular water molecule in the first coordination

(24) Connick, R. E.; Fiat, D. N. *J. Chem. Phys.* **1963**, *39*, 1349.(25) Alei, M.; Jackson, J. A. *J. Chem. Phys.* **1964**, *41*, 3402.(26) (a) Yamaguchi, T.; Ohtaki, H.; Spohr, E.; Palinkas, G.; Heinzinger, K.; Probst, M. M. *Z. Naturforsch.* **1986**, *A41*, 1175. (b) Probst, M. M.; Spohr, E.; Heinzinger, K. *Chem. Phys. Lett.* **1989**, *161*, 405.(27) Plumb, W.; Harris, G. M. *Inorg. Chem.* **1964**, *3*, 542.(28) Fiat, D.; Connick, R. E. *J. Am. Chem. Soc.* **1968**, *90*, 608.(29) Swift, T. J.; Fritz, O. G.; Stephenson, T. A. *J. Chem. Phys.* **1967**, *46*, 406.(30) Fiat, D.; Connick, R. E. *J. Am. Chem. Soc.* **1966**, *88*, 4754.

Table IV. Rate Constants, Activation Parameters, and Mechanisms for Solvent S Exchange on $[\text{BeS}_4]^{2+}$ in Neat Solvent and in CD_3NO_2 as Diluent (ClO_4^- as Counterion)

solvent	$k_{\text{ex}}^{298\text{ a}}/\text{s}^{-1}$	$k_1^{298\text{ b}}/\text{s}^{-1}$	$k_2^{298\text{ b}}/\text{kg mol}^{-1}\text{ s}^{-1}$	$\Delta H^\ddagger/\text{kJ mol}^{-1}$	$\Delta S^\ddagger/\text{J K}^{-1}\text{ mol}^{-1}$	$\Delta V^\ddagger/\text{cm}^3\text{ mol}^{-1}$	mech	ref
H ₂ O	730 ^c			59.2	+8.4	-13.6	A	this work
DMSO			213	35.0	-83.0	-2.5	A, I _a	this work
			140 ^d	51.1	-32.3		A, I _a	3
	230 ^e			25	-110		A, I _a	4
TMP			4.2	43.5	-87.1	-4.1	A, I _a	this work
			1.5 ^d	56.0	-54.0		A, I _a	5
	4.9			70.3	+3.5		?	6
DMMP ^f			0.81 ^d	60.2	-44.4		A, I _a	5
	2.6			73.1	+8.5		?	7
MMPP ^f			0.22 ^d	68.7	-26.1		A, I _a	7
DMF		0.2	16	52.0	-47.5	-3.1	A, I _a	this work
			8.5 ^d	74.9	-7.3		D	this work
		0.1		58.1	-32.0		A, I _a	8
	68 ^{g,h}			83.6	+16.3		D	8
NMA ^f			0.32 ^d	54.8	-26.1		i	8
		0.23		76.8	+3.1		A, I _a	8
				71.5	-17.3		D	8
DMA ^f			0.34 ^d	66.7	-30.1		A, I _a	8
		0.38		56.9	-62.1		D	8
DEA ^f			0.59 ^d	68.5	-19.6		A, I _a	9
		0.044		76.4	-14.6		D	9
DMADMP ^f		7.3×10^{-3}		89.1	+12.6		D	5
TMU		1.0		79.6	+22.3	+10.5	D	this work
		1.4		77.1	+16.4		D	3
DMPU		0.1		92.6	+47.5	+10.3	D	this work

^a In neat solvent. ^b In CD_3NO_2 as diluent. ^c Previous studies lead to values of $k_{\text{ex}}^{298} = 2100, 1800\text{ s}^{-1}$, $\Delta H^\ddagger = 34.7, 41.5\text{ kJ mol}^{-1}$, and $\Delta S^\ddagger = -63, -44\text{ J K}^{-1}\text{ mol}^{-1}$ (refs 12, 13 respectively). ^d $k_2/\text{dm}^3\text{ mol}^{-1}\text{ s}^{-1}$ ($\approx 0.88k_2/\text{kg mol}^{-1}\text{ s}^{-1}$). ^e NO_3^- as counterion. ^f DMMP = dimethyl methylphosphonate, MMPP = methyl methylphenylphosphinate, NMA = *N*-methylacetamide, DMA = *N,N*-dimethylacetamide, DEA = *N,N*-diethylacetamide, DMADMP = *O,O'*-dimethyl *N,N*-dimethylphosphoramidate. ^g Average of the formyl (66, 53.9, -29.3) and *N*-methyl (70, 55.7, -22.9) resonance data. ^h Previous study leads to values of $k_{\text{ex}}^{298} = 310\text{ s}^{-1}$, $\Delta H^\ddagger = 61.1\text{ kJ mol}^{-1}$, and $\Delta S^\ddagger = +10.9\text{ J K}^{-1}\text{ mol}^{-1}$.¹⁰ ⁱ The k_{ex} value obtained in DMF alone is considerably greater than k_1 observed in nitromethane, which may indicate the operation of an A (or I_a) mechanism by itself or in parallel with a D mechanism.⁸

sphere of the metal ion in the neat solvent and $1/T_{2Q}^b$ is the quadrupolar relaxation rate. The temperature dependence of k_{ex} was expressed by the Eyring equation. An Arrhenius temperature behavior was assumed for the quadrupolar relaxation rate, eq 5,¹⁶

$$1/T_{2Q}^b = (1/T_{2Q}^b)^{298} \exp[E_Q^b/R(1/T - 1/298.15)] \quad (5)$$

where $(1/T_{2Q}^b)^{298}$ is the relaxation rate at 298.15 K and E_Q^b is the activation energy. It is obvious from Figure 4 that the measured $1/T_2^b$ is dominated by the quadrupolar relaxation ($1/T_{2Q}^b$) at low temperatures and by the solvent exchange (k_{ex}) at high temperatures. As no influence of acidity on $1/T_2^b$ has been detected, we used the mean value of $1/T_2^b$ obtained for three solutions ($[\text{H}^+] = 0.10, 0.20, \text{ and } 0.38\text{ mol kg}^{-1}$). The fit of eqs 4 and 5 and the Eyring equation to these data lead to $k_{\text{ex}}^{298} = 733 \pm 56\text{ s}^{-1}$, $\Delta H^\ddagger = 59.2 \pm 1.5\text{ kJ mol}^{-1}$, $\Delta S^\ddagger = +8.4 \pm 4.5\text{ J K}^{-1}\text{ mol}^{-1}$, $E_Q^b = 17.2 \pm 2.2\text{ kJ mol}^{-1}$, and $(1/T_{2Q}^b)^{298} = 739 \pm 61\text{ s}^{-1}$. Three supplementary values of $1/T_2^b$ at high temperature, obtained from the most acidic solution, were included in this fit (see Figure 4).

Pressure Dependence of Water Exchange. The pressure dependence of $\ln k_{\text{ex}}$ can be described by the linear equation (6),

$$\ln(k_{\text{ex}})_P = \ln(k_{\text{ex}})_0 - P\Delta V^\ddagger/RT \quad (6)$$

since we can assume that the volume of activation (ΔV^\ddagger) is pressure independent, as is usually the case for simple water-exchange reactions,³¹ $(k_{\text{ex}})_0$ being the exchange rate at zero pressure. A similar equation, eq 7, describes the pressure dependence of

$$\ln(1/T_{2Q}^b)_P = \ln(1/T_{2Q}^b)_0 - P\Delta V_Q^\ddagger/RT \quad (7)$$

the quadrupolar relaxation rate, which leads to the activation volume ΔV_Q^\ddagger of the quadrupolar relaxation and to the quadrupolar relaxation rate at zero pressure $(1/T_{2Q}^b)_0$. As no effect of acidity has been detected at any temperature, $1/T_2^b$ was determined up

to 210 MPa for a solution with $[\text{H}^+] = 0.4\text{ m}$, corresponding to the most acidic sample used in the temperature study. Measurements at high (321.2 and 330.2 K) and low temperatures (273.9 and 277.8 K) allow the accurate determination of the pressure dependence of both the exchange and quadrupolar relaxation rates. Equations 4, 6, and 7 were simultaneously nonlinear least-squares fitted to the whole set of experimental $1/T_2^b$ data (Figure 5), leading to $\Delta V^\ddagger = -13.6 \pm 0.5\text{ cm}^3\text{ mol}^{-1}$, $\Delta V_Q^\ddagger = +0.3 \pm 0.5\text{ cm}^3\text{ mol}^{-1}$, $(k_{\text{ex}}^{321})_0 = 3594 \pm 100\text{ s}^{-1}$, $(k_{\text{ex}}^{330})_0 = 7937 \pm 209\text{ s}^{-1}$, $(1/T_{2Q}^b)^{274}_0 = 1321 \pm 37\text{ s}^{-1}$, and $(1/T_{2Q}^b)^{278}_0 = 1169 \pm 33\text{ s}^{-1}$. In the fitting procedure the following parameters, too small to be adjusted, were fixed to the values calculated from the variable-temperature activation parameters obtained above: $(1/T_{2Q}^b)^{321}_0 = 499\text{ s}^{-1}$, $(1/T_{2Q}^b)^{330}_0 = 377\text{ s}^{-1}$, $(k_{\text{ex}}^{274})_0 = 81\text{ s}^{-1}$, and $(k_{\text{ex}}^{278})_0 = 119\text{ s}^{-1}$.

Discussion

Nonaqueous Solvent Exchange. Previous NMR studies have shown that the solvent exchanges on the small tetrahedrally coordinated Be^{2+} ion in noncoordinating diluents (eq 1) occur through a first-order path (k_1) characterizing a dissociative (D) mechanism and/or a second-order path (k_2) characterizing an associative (A) or an interchange (I) mechanism (see eq 2 and Table IV). Our variable-temperature results and rate law determinations confirm the experimental data obtained previously for DMSO,³ TMP,⁵ DMF,⁸ and TMU³ in the diluent nitromethane.

For TMU and DMPU the rate law is first order, and the ΔS^\ddagger and ΔV^\ddagger values are clearly positive. The conjunction of these facts indicates the occurrence of a D mechanism. From the first-order rate law, the same mechanism is assumed for DMADMP.⁵

For DMSO, TMP, DMMP, and MMPP the second-order rate law does not allow one to distinguish between an A mechanism and an I mechanism. For the latter the activation mode may vary from predominantly dissociative (I_d) to predominantly associative (I_a): first, an encounter complex, of formation constant K_{08} , is formed with the entering ligand residing in the second coordination sphere of BeS_4^{2+} , and second, the synchronous rate-determining

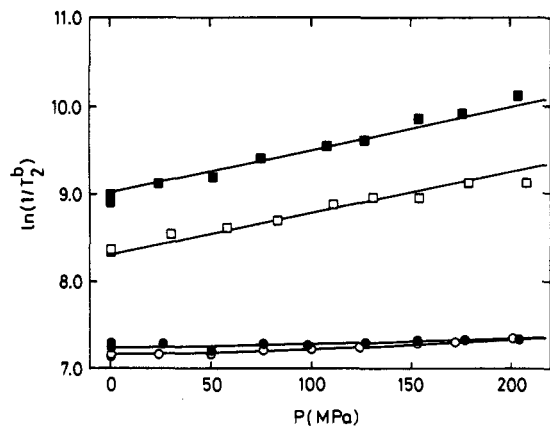


Figure 5. Pressure dependence of the transverse relaxation rate, $1/T_2^b$, of the bound- H_2O ^{17}O NMR signal of $0.10 \text{ mol kg}^{-1} \text{ Be}(\text{H}_2\text{O})_4^{2+}$ in 44% ^{17}O -enriched water, with $0.40 \text{ mol kg}^{-1} \text{ HClO}_4$ and 0.10 mol kg^{-1} added $\text{Mn}(\text{ClO}_4)_2$ in the exchange (\blacksquare , 330 K; \square , 321 K) and the quadrupolar (\bullet , 274 K; \circ , 278 K) regions (measured at 27.11 MHz).

interchange between the entering and leaving ligands occurs. In this frame the k_2 term of eq 2 is equal, if the encounter complex forms in negligible proportion, to $K_{\text{eq}}k_1$ where k_1 is the rate constant for the interchange step. This equality can be derived with respect to pressure leading to $\Delta V_2^\ddagger = \Delta V_{\text{os}}^\ddagger + \Delta V_1^\ddagger$, an expression relating the experimentally measured activation volume to the reaction volume for the formation of the encounter complex and the activation volume for the interchange step, respectively. Fortunately, according to the Hemmes equation,³² $\Delta V_{\text{os}}^\ddagger$ is equal to zero (+2 and 0 charged species), and therefore the sign of ΔV_2^\ddagger is immediately a diagnostic of the activation step: positive when bond breaking is favored or negative when bond making is favored. The negative ΔS^\ddagger values, and especially the negative ΔV^\ddagger for DMSO and TMP, suggest an associative activation mode for those solvent exchanges. However the small absolute value for ΔV^\ddagger does not allow the distinction between an I_a and an A mechanism. In the latter case, one may well imagine a large negative contribution due to bond formation, partially compensated by a positive contribution due to bond lengthening of the nonexchanging solvent molecules in a sterically crowded five-coordinate intermediate.

The amide solvent (DMF, NMA, DMA, and DEA) exchanges on Be^{2+} occur through two simultaneous paths in nitromethane as diluent. Similar to the case of the urea ligand exchanges discussed above, the k_1 term of the rate law is consistent with the operation of a D mechanism. The k_2 term is consistent with the operation of either an A or an I_a mechanism; this has been discussed in detail by Lincoln et al.^{8,9} in terms of the effect of steric hindrance and electron-donating power of the solvent and its propensity to exchange through the k_1 and k_2 paths. From these considerations there is persuasive evidence for the operation of an A or an I_a mechanism for the k_2 exchange path. This is now further supported by the $-3.1 \text{ cm}^3 \text{ mol}^{-1}$ activation volume value determined for the k_2 exchange path in the DMF case.

On the basis of these data, it appears that solvent crowding stabilizes a three-coordinate intermediate (D mechanism) relative to a five-coordinate transition state (I_a) or intermediate (A). Similar conclusions were also reached in the case of acetonitrile^{3,7-9} and dichloromethane⁶⁻⁸ as diluent. In neat solvent^{4,6-8} the mechanistic conclusions, due to the nonavailability of rate laws, are not always as conclusive.

Water Exchange. In principle the water exchange around a metal ion could be studied by either ^1H or ^{17}O NMR spectroscopy, both nuclei belonging to the water molecule. However, it has been shown that the proton-exchange rates in general are complicated by the fact that not only water molecule exchange but also proton transfer due to protolytic dissociation of the aqua ion contribute to the total rate. Frahm et al.¹³ have shown that the protolytic dissociation of the aquaberyllium(II) ion as measured by ^1H NMR

spectroscopy is approximately 1 order of magnitude faster than water exchange as measured by ^{17}O NMR spectroscopy. Further, the water-exchange rate itself can be strongly enhanced in hydrolyzed aqua ions. For example water exchange in $[\text{M}(\text{H}_2\text{O})_5(\text{OH})]^{2+}$ is 2–3 orders of magnitude faster than in $[\text{M}(\text{H}_2\text{O})_6]^{3+}$ ($\text{M} = \text{Ga}, \text{Fe}, \text{Cr}, \text{Ru}$),¹¹ and even in some cases, such as for $\text{Fe}(\text{III})$,^{33,34} there is a complete mechanism changeover from I_a to I_a , respectively. According to those two reasons, our study was performed by using ^{17}O NMR spectroscopy and at variable acidity, between 0.1 and $0.4 \text{ mol kg}^{-1} \text{ HClO}_4$: no effect of this variation could be detected on the rate constant k_{ex} . The sensible difference between our k_{ex}^{298} , ΔH^\ddagger , and ΔS^\ddagger values and those previously reported (see Table IV) may be due to the absence of added acid,^{12,13} the much higher ionic strength used ($\mu = 18.5 \text{ mol kg}^{-1}$ ¹² and 10.8 mol kg^{-1} ,¹³ compared to 1.0 mol kg^{-1}), and the assumption of equal spin-spin relaxation rates¹³ for the bound and free ^{17}O nuclei (at 298 K: $1/T_{2Q}([\text{Be}(\text{H}_2\text{O})_4]^{2+}) = 739 \text{ s}^{-1}$ and $1/T_{2Q}(\text{H}_2\text{O}) \approx 150 \text{ s}^{-1}$ ³⁵) in the former studies.

In this study of water exchange on $[\text{Be}(\text{H}_2\text{O})_4]^{2+}$ in neat solvent, no rate law is available and one has to rely on the activation parameters ΔS^\ddagger and ΔV^\ddagger for mechanistic assignments. ΔS^\ddagger , close to zero, is not an infallible mechanistic indicator.^{37,38} On the other hand, the ΔV^\ddagger value of $-13.6 \text{ cm}^3 \text{ mol}^{-1}$, the most negative ever obtained for water exchange at a metal ion, is clearly indicating an associative activation mode. However it is more difficult to decide whether an I_a or an A mechanism is operative, because the activation volume $\Delta V_{\text{lim}}^\ddagger(\text{A})$ for the limiting mechanism is unknown. A first approximation, neglecting bond elongation of the nonreacting water molecules, is to take the value of the partial molar volume of a water molecule electrostricted in the second coordination sphere, which can be estimated to be $-15 \text{ cm}^3 \text{ mol}^{-1}$.³⁹ A second alternative, suggested by Swaddle,⁴⁰ is to take for $\Delta V_{\text{lim}}^\ddagger(\text{A})$ the difference between the partial molar volumes V_{abs}^0 of the aqua ion of increased coordination number (A mechanism) or decreased coordination number (D mechanism) and that of the aqua ion in its initial state. These partial molar volumes can be estimated by using the semiempirical equation⁴⁰ (8), where r

$$V_{\text{abs}}^0 = 2.523 \times 10^{-6}(r + 238.7)^3 + 18.07n_c - 417.5z^2(r + 238.7) \quad (8)$$

is the ionic radius (in pm), z the charge of the cation, and n_c the number of water molecules in the first coordination sphere. Using the Shannon⁴¹ $r_3 = 16 \text{ pm}$, $r_4 = 27 \text{ pm}$, and $r_5 = 36 \text{ pm}$ (average between r_4 and $r_6 = 45 \text{ pm}$) values for Be^{2+} , one calculates $\Delta V_{\text{lim}}^\ddagger(\text{A}) = -12.9 \text{ cm}^3 \text{ mol}^{-1}$. The near identity between the experimental and the calculated values allows one to conclude an A mechanism for water exchange on $[\text{Be}(\text{H}_2\text{O})_4]^{2+}$. This conclusion is the same as that reached for the water exchange on $[\text{Ti}(\text{H}_2\text{O})_6]^{3+}$ with an experimental value of $-12.1 \text{ cm}^3 \text{ mol}^{-1}$,¹¹ the most negative obtained for an octahedral aqua ion.

In conclusion, the assignment of an A mechanism for the small water molecule confirms that a sterically governed mechanistic crossover is taking place for solvent exchange on the small Be^{2+} ion, as previously observed for solvent exchange on Mn^{2+} .⁴²

Acknowledgment. We thank Urban Frey and Pascal Gübeli for their participation in some NMR measurements and the Swiss National Science Foundation for supporting this research under Grant No. 2.672-0.87.

- (33) Swaddle, T. W.; Merbach, A. E. *Inorg. Chem.* **1981**, *20*, 4212.
 (34) Grant, M.; Jordan, R. B. *Inorg. Chem.* **1981**, *20*, 55.
 (35) Obtained at 297 K, for a solution of $[\text{Eu}(\text{ClO}_4)_3] = 0.28 \text{ m}$ in 4.6% ^{17}O -enriched H_2O with 1.95 m HClO_4 .³⁶
 (36) Cossy, C. Ph.D. Thesis, University of Lausanne, Switzerland, 1986.
 (37) Swaddle, T. W. *Coord. Chem. Rev.* **1974**, *14*, 217.
 (38) Newman, K. E.; Meyer, F. K.; Merbach, A. E. *J. Am. Chem. Soc.* **1979**, *101*, 1470.
 (39) Stranks, D. R. *Pure Appl. Chem.* **1974**, *38*, 303.
 (40) Swaddle, T. W. *Inorg. Chem.* **1983**, *22*, 2663.
 (41) Shannon, R. D. *Acta Crystallogr., Sect. A* **1976**, *A32*, 751.
 (42) Cossy, C.; Helm, L.; Merbach, A. E. *Helv. Chim. Acta* **1987**, *70*, 1516.

(32) Hemmes, P. J. *Phys. Chem.* **1972**, *76*, 895.

Supplementary Material Available: First- and second-order rate constants, k_1 and k_2 , respectively, for solvent S exchange on BeS_4^{2+} in CD_3NO_2 as diluent, at variable pressure (Table SI), relaxation rates, $1/T_2^b$, of the bound-water ^{17}O NMR signal of $[\text{Be}(\text{H}_2\text{O})_4]^{2+}$ in ^{17}O -en-

riched water as a function of temperature (Table SII) and pressure (Table SIII), and elementary analyses of the nonaqueous solvates (Table SIV) (3 pages). Ordering information is given on any current masthead page.

Contribution from the Department of Chemistry,
Purdue University, West Lafayette, Indiana 47907

Non-Metal Redox Kinetics: Reactions of Sulfite with Dichloramines and Trichloramine

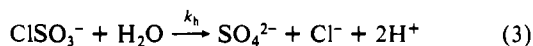
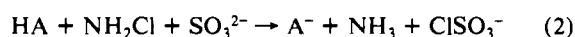
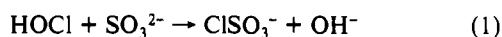
Boudin S. Yiin and Dale W. Margerum*

Received September 14, 1989

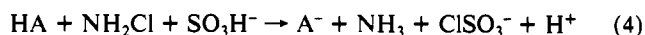
Pulsed-accelerated-flow (PAF) and stopped-flow techniques are used to study the kinetics of HNCl_2 and CH_3NCl_2 reactions with sulfite. Pseudo-first-order rate constants with excess sulfite at $\text{p}[\text{H}^+]$ 3.7–6.4 are measured from 35–45 000 s^{-1} (25.0 °C, $\mu = 0.50$). Acid suppresses the rate because SO_3H^- is much less reactive than SO_3^{2-} . The rate expression is $-\text{d}[\text{RNCl}_2]/\text{d}t = k_1[\text{RNCl}_2][\text{SO}_3^{2-}]$, where k_1 ($\text{M}^{-1}\text{s}^{-1}$) is 5.8×10^6 for HNCl_2 and 2.4×10^7 for CH_3NCl_2 . The initial nitrogen product is RNHCl , which reacts further with sulfite. Trichloramine reactions with sulfite are measured by the PAF method under second-order conditions with unequal concentrations (25.0 °C, $\mu = 0.50$) from $\text{p}[\text{H}^+]$ 3.8 to 4.6. The rate expression is $-\text{d}[\text{NCl}_3]/\text{d}t = (k_1[\text{SO}_3^{2-}] + k_2[\text{SO}_3\text{H}^-])[\text{NCl}_3]$, where k_1 is $4.5 \times 10^9 \text{ M}^{-1}\text{s}^{-1}$ and k_2 is $1.4 \times 10^7 \text{ M}^{-1}\text{s}^{-1}$. The initial nitrogen product is HNCl_2 , which reacts further with sulfite. A Cl^+ -transfer mechanism is proposed for all the reactions with sulfite to give ClSO_3^- as an initial product that hydrolyzes to give Cl^- and SO_4^{2-} . The relative reactivities of active chlorine species with SO_3^{2-} are $\text{NCl}_3 \gg \text{HNCl}_2 \gg \text{NH}_2\text{Cl} \ll \text{OCl}^-$, where the NCl_3 and HNCl_2 reactions are suppressed by acid whereas the NH_2Cl and OCl^- reactions are acid assisted.

Introduction

Sulfite, hydrogen sulfite, and sulfur dioxide are well-known as chlorinating agents that remove or reduce the chlorine residuals (OCl^- , HOCl , NH_2Cl , HNCl_2 , NCl_3) in coolant water and waste water.¹ All these chlorine species react relatively rapidly with sulfite, but there are great differences in the magnitude of the rate constants and in their rate expressions. The second-order rate constant for the reaction of OCl^- with SO_3^{2-} is $2.3 \times 10^4 \text{ M}^{-1}\text{s}^{-1}$ (25.0 °C, $\mu = 0.50$),² while the corresponding value for NH_2Cl with SO_3^{2-} is only $7.7 \text{ M}^{-1}\text{s}^{-1}$.³ These rate constants are appropriate for reactions at high pH; however, the observed rate constants for the hypochlorite reaction increase greatly below pH 12. The reactivity of HOCl ($\text{p}K_a = 7.50$, $\mu = 0.50$) with SO_3^{2-} is 3.3×10^4 times greater than that of OCl^- ($k_{\text{HOCl}} = 7.6 \times 10^8 \text{ M}^{-1}\text{s}^{-1}$).² Similarly, the rate of the chloramine reaction with SO_3^{2-} increases greatly below pH 10 and the reaction is general-acid assisted by NH_4^+ , $\text{B}(\text{OH})_3$, H_2PO_4^- , H_3O^+ , and other acids (HA).³ The Brønsted α value is 0.71, and the third-order rate constant for $\text{H}_3\text{O}^+ + \text{NH}_2\text{Cl} + \text{SO}_3^{2-}$ is $8 \times 10^{10} \text{ M}^{-2}\text{s}^{-1}$. The corresponding third-order rate constant for $\text{H}_3\text{O}^+ + \text{OCl}^- + \text{SO}_3^{2-}$ is $2.4 \times 10^{16} \text{ M}^{-2}\text{s}^{-1}$. Thus, the relative reactivity is $\text{OCl}^- \gg \text{NH}_2\text{Cl}$ and both reactions with SO_3^{2-} are strongly acid assisted. These are Cl^+ -transfer reactions, where chlorosulfate is the initial product (eqs 1 and 2). The hydrolysis of ClSO_3^- (eq 3) is also rapid, and the k_h value at 25.0 °C is 270 s^{-1} .⁴

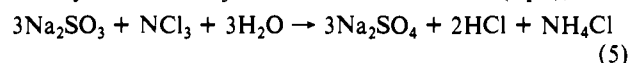


Rate constants have also been resolved for the general-acid-assisted reactions of chloramine with hydrogen sulfite (eq 4).³ The



rate constant for $\text{H}_3\text{O}^+ + \text{NH}_2\text{Cl}$ with SO_3^{2-} is larger than the corresponding rate constant with SO_3H^- by a factor of 220. This reflects the stronger nucleophilicity of SO_3^{2-} compared to SO_3H^- . However, the overall effect of increased acid concentration is to increase the reaction rate. The observed second-order rate constant for NH_2Cl with total sulfite ($[\text{SO}_3^{2-}]_{\text{T}} = [\text{SO}_3^{2-}] + [\text{SO}_3\text{H}^-]$) increases by nearly 5 orders of magnitude from pH 10 to pH 3.³

Many years ago Dowell and Bray⁵ showed that sulfite quantitatively reduces NCl_3 to ammonia and chloride (eq 5), while



other reducing agents cause some evolution of N_2 . Our work demonstrates the stepwise nature of this reaction and the intermediate formation of HNCl_2 , NH_2Cl , and ClSO_3^- .

In the present study we examine the kinetics of reactions of two dichloramines (HNCl_2 and CH_3NCl_2) and of trichloramine (NCl_3) with sulfite. The reactions are very rapid and require stopped-flow or pulsed-accelerated-flow (PAF)⁶⁻⁸ techniques. We find that acid suppresses the reaction rates because of the much greater reactivity of SO_3^{2-} compared to SO_3H^- and because the reactions are not acid catalyzed. The sequence of reactions that occur for NCl_3 with SO_3^{2-} is given in eqs 6 and 7. This is followed



by the reactions in eqs 2–4. The measurement of rate constants for the NCl_3 reaction is a difficult challenge. It requires use of the PAF technique in the UV region where only NCl_3 absorbs and low concentrations are needed with second-order unequal conditions. Nevertheless, we are able to resolve the second-order rate constants for the reactions of SO_3^{2-} and SO_3H^- with NCl_3 .

- Chen, A. M.; Skochdopole, J.; Koski, P.; Cole, L. *Science* **1980**, *207*, 90–92.
- Fogelman, K. D.; Walker, D. M.; Margerum, D. W. *Inorg. Chem.* **1989**, *28*, 986–993.
- Yiin, B. S.; Walker, D. M.; Margerum, D. W. *Inorg. Chem.* **1987**, *26*, 3435–3441.
- Yiin, B. S.; Margerum, D. W. *Inorg. Chem.* **1988**, *27*, 1670–1672.

- Dowell, C. T.; Bray, W. C. *J. Am. Chem. Soc.* **1917**, *39*, 896–905.
- Jacobs, S. A.; Nemeth, M. T.; Kramer, G. W.; Ridley, T. Y.; Margerum, D. W. *Anal. Chem.* **1984**, *56*, 1058–1065.
- Nemeth, M. T.; Fogelman, K. D.; Ridley, T. Y.; Margerum, D. W. *Anal. Chem.* **1987**, *59*, 283–291.
- Bowers, C. P.; Fogelman, K. D.; Nagy, J. C.; Ridley, T. Y.; Wang, Y. L.; Evetts, S. W.; Margerum, D. W. To be submitted for publication.